

# Comparison of Spherical Antennas Fabricated via Conformal Printing: Helix, Meanderline, and Hybrid Designs

Jacob J. Adams, *Member, IEEE*, Scott C. Slimmer, Thomas F. Malkowski, Eric B. Duoss, Jennifer A. Lewis, and Jennifer T. Bernhard, *Fellow, IEEE*

**Abstract**—The design tradeoffs between three spherically conformal electric monopoles—the spherical helix (SH), spherical meanderline (SM), and a hybrid design—are explored through both simulation and measurement. We show that the SH is efficient, but can be difficult to impedance match without external components. On the other hand, the SM antenna has a widely controllable impedance with slightly increased loss. Thus, a hybrid design is proposed that retains the desirable qualities of both the SH and SM. All three designs are fabricated using a conformal printing technique for comparison. We describe the design tradeoffs and physical insights gained through evaluating the efficiency,  $Q$ , and matching behavior of these antennas.

**Index Terms**—Conformal printing, electrically small, impedance matching, quality factor, spherical antenna.

## I. INTRODUCTION

WHEELER realized early on that the performance of an electrically small antenna (ESA) is related to its occupied volume [1]. The prevailing performance metric for ESAs is the quality factor ( $Q$ ), which has a lower bound determined by physics for a fixed antenna size. The quality factor is inversely proportional to the antenna's matched bandwidth when the antenna has a single resonance [2].

For antennas consisting of only metal and dielectrics, a spherical volume supporting the electric dipole radiation ( $TM_{10}$  spherical mode) exhibits the lowest  $Q$  for a given maximum dimension [3]. The lower bound for this  $TM_{10}$  mode radiator

Manuscript received October 05, 2011; revised November 07, 2011; accepted November 19, 2011. Date of publication December 09, 2011; date of current version December 26, 2011. The work of J. J. Adams and S. C. Slimmer is supported by the Intelligence Community Postdoctoral Research Fellowship Program. This work was supported in part by the US Department of Energy (DOE), Division of Materials Sciences, under Award DE-FG02-07ER46471.

J. J. Adams and J. T. Bernhard are with the Electromagnetics Laboratory, Department of Electrical and Computer Engineering, University of Illinois, Urbana, IL 61801 USA (e-mail: jjadams@illinois.edu; jbernarh@illinois.edu).

S. C. Slimmer and J. A. Lewis are with the Frederick Seitz Materials Research Laboratory, Department of Materials Science and Engineering, University of Illinois, Urbana, IL 61801 USA (e-mail: slimmer@illinois.edu; jalewis@illinois.edu).

T. F. Malkowski is with the Department of Materials Science, University of California, Santa Barbara, CA 93106 USA (e-mail: tmalkowski@umail.ucsb.edu).

E. B. Duoss is currently with the Center for Micro- and Nano-Technology, Lawrence Livermore National Laboratory, Livermore, CA 94550 USA (e-mail: duoss1@llnl.gov).

Color versions of one or more of the figures in this letter are available online at <http://ieeexplore.ieee.org>.

Digital Object Identifier 10.1109/LAWP.2011.2178999

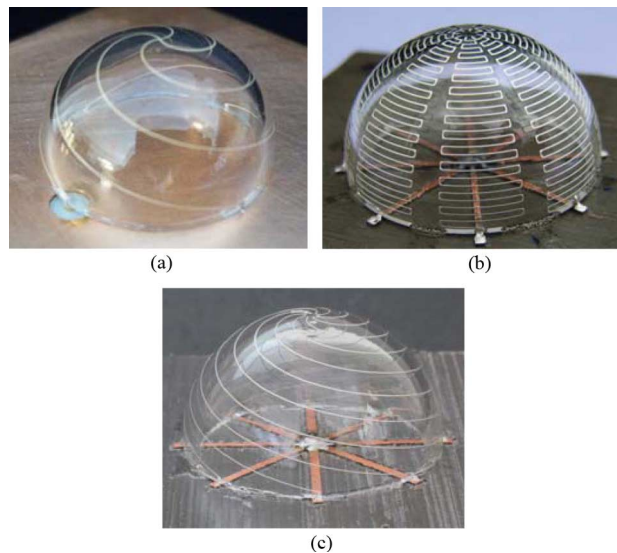


Fig. 1. Photographs of the fabricated SH, SM, and hybrid (H) antennas. (a) Spherical helix (SH4). (b) Spherical meanderline (SM8). (c) Hybrid (H8).

was first tabulated in [3], and an approximate expression was calculated in [4] as

$$Q_{\min, TM_{10}} \approx \eta_r \left( \frac{3}{2(ka)^3} + \frac{3}{5ka} \right) \quad (1)$$

where  $\eta_r$  is the radiation efficiency,  $k$  is the wavenumber at the center frequency, and  $2a$  is the maximum dimension of the antenna.

The advantage of a space-filling, spherical volume in achieving the minimum  $Q$  has been demonstrated experimentally. Two recent spherical antennas with  $Q$  approaching the lower bound are the spherical helix (SH) [5], [6] and spherical meanderline (SM) [7] antennas. The SH [Fig. 1(a)] consists of several wires coiled into a helix along a spherical surface and exhibits a resonant input impedance in the electrically small region. One arm is fed, and the others are shorted to ground. While it can be designed to radiate with either linear or elliptical polarization, this letter focuses on the case of linear polarization. The SM [Fig. 1(b)] is specifically designed to support the  $J_\theta = \sin(\theta)$  current distribution of the  $TM_{10}$  spherical mode [3], [8]. Several radiating arms are meandered along the spherical surface to create the appropriate sinusoidal

distribution in  $\theta$ . The SM design is widely tunable for differing  $ka$  values, frequencies, and system impedances using a matching technique introduced in [8].

The SH and SM antennas are both small electric monopoles with conductors occupying a hemispherical surface. However, the two antennas use different approaches for impedance matching and wire layout to induce self-resonance. Since either design can be fabricated via conformal printing of silver ink [7], some questions arise as to the benefits of each design and whether one configuration is better suited than the other. In Section II, we compare the matching techniques used in these antennas, and in Section III, we evaluate their efficiency and  $Q$ . From these comparisons, it will be clear that the SH structure is a more efficient radiator, but its feeding technique results in a limited set of impedances that can be designed. While the SM has more loss, it has a versatile impedance match that can be fine-tuned with ease.

Thus, in this letter, we introduce a hybrid design [Fig. 1(c)] by taking the efficient radiating structure of the SH and combining it with the independent impedance control found in the SM design. The resulting hybrid (H) design retains the desirable qualities of the SH and SM. The hemispherical portion of the hybrid remains largely the same as the SH except at the apex, where the arms are disconnected to prevent the excitation of inductive modes. Then, similarly to the SM, the hemisphere is placed on a thin planar dielectric that can be used to control the impedance match. All three antennas couple strongly to the  $TM_{10}$  spherical mode, and they exhibit the radiation pattern of a short monopole. Since they excite the same mode, their overall  $Q$  is similar, approaching the lower bound. However, we investigate other performance differences that arise from using different radiators and matching techniques.

## II. IMPEDANCE MATCHING

Many ESAs have highly reactive input impedances and large mismatch losses that require a narrowband lumped element matching network. In contrast, most of the antennas discussed in this letter are designed to be impedance-matched in the electrically small region, requiring no external components. The exception to this is the spherical helix, which cannot always be matched.

We used HFSS to impedance match the SH, SM, and H antennas. To facilitate direct comparison to measurements, four- and eight-arm antennas were simulated using typical glass hemisphere dimensions ( $\epsilon_r = 4.6$ , outer radius = 12.7 mm, thickness = 1.3 mm). The cross section of the printed conductive ink is assumed to be  $100 \times 20 \mu\text{m}^2$  with conductivity of  $2 \times 10^7$  S/m [7]. The SM and H antennas require a thin planar dielectric substrate, and 0.025-in Duroid 6002 was used for simulations. The antennas were tuned to be self-resonant at several discrete electrical sizes. In the case of the eight-arm SH, it was tuned to have a reflection coefficient minimum since it was not self-resonant. Tuning for the antennas was accomplished by increasing the length of the wires to decrease the resonant frequency, and vice versa.

Fig. 2 shows the length of wire needed to achieve self-resonance at a particular electrical size. The SH and H antennas require slightly more wire length than would be required for a

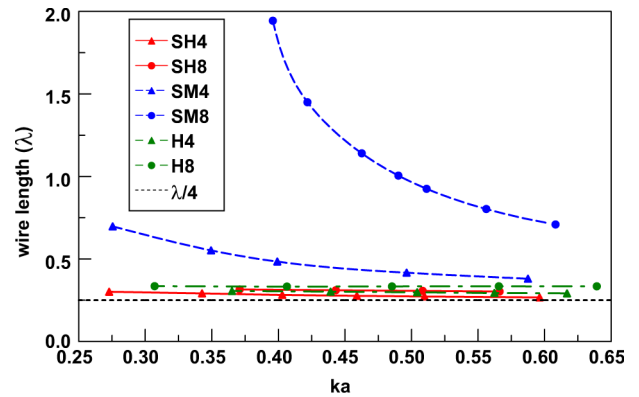


Fig. 2. Simulated length of wire (normalized to one wavelength) per arm required for operation at a particular electrical size. Results are given for four- and eight-arm variations of the SH, SM, and H antennas. A quarter-wavelength is shown for reference.

self-resonant straight monopole ( $\approx \lambda/4$ ). Since the hybrid and SH designs have a similar radiator, they require similar wire length to operate at a particular electrical size. On the other hand, it is clear that the SM antennas require significantly more wire length than the other designs to achieve the same resonant frequency. This difference between the SH and SM designs is due to the differing arrangement of conductors on the hemisphere. The SM antenna has strongly coupled currents flowing in opposite directions, so more wire is needed to achieve a particular resonant frequency [9]. Because of this increased coupling, the difference is greatest at small electrical sizes and when there are many arms. Thus, eight-arm SM designs with  $ka < 0.4$  become very challenging to both simulate and fabricate.

Self-resonance in itself is not a guarantee of a good impedance match; the antenna must also present the appropriate input resistance at resonance. ESAs typically have a small resonant resistance due to high currents at the feed point when a single mode is present in the structure [10], but there are several ways to increase this impedance.

A shorted stub is commonly used to raise the input resistance to an acceptable level [e.g., the folded dipole and planar inverted-F antenna (PIFA)]. Because the stub is shorted, the feed point current of the radiating mode is reduced, raising its impedance [11]. Loop-like modes are also excited and present inductive susceptance in parallel to the radiating mode. Best uses this inductive or “folding” approach to increase the SH’s resistance from a few ohms to hundreds of ohms [5]. The structure is fed from one arm, and the others are shorted to ground. However, because the portion of the SH that supports the radiating mode (the spiral arms) also supports the inductive matching mode, it is difficult to control the modes independently. The result is that for particular combinations of electrical size and number of arms, the impedance is largely fixed. The choices of input resistance at a particular frequency are discrete since they are set by the number of arms.

In contrast, the SM antenna uses a capacitive matching approach where the radiating mode and a higher-order mode are controlled independently to cause an antiresonance with a highly adjustable resistance. This is done by placing the antenna on a thin planar substrate with copper feed lines in a star-like pattern that is fed in the center [8], [10]. The higher-order

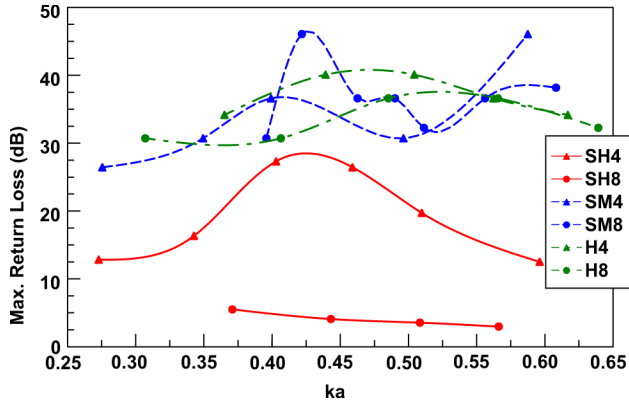


Fig. 3. Simulated maximum return loss (at the operating frequency) of the SH, SM, and H antenna designs when connected directly to a 50- $\Omega$  line.

mode resonates at a frequency above the antenna's operating frequency and contributes a capacitive susceptance. The value of this susceptance can be adjusted via both the feed lines and the substrate properties yielding extra degrees of freedom relative to the SH. This resolves the problem of "forbidden" impedances, and a continuous range of impedances from a few ohms to several kilo-ohms can be realized via the superposition of the modes.

Fig. 3 illustrates the benefit of this independent impedance control. The maximum return loss of the SM and H antennas is significantly higher than the return loss of the SH antennas. The SH8 antenna has particularly low return loss that will decrease further as more arms are added. Placing the hemispherical helix on the planar substrate and shifting the feed from one arm to the center of the substrate yields significantly improved return loss for the hybrid.

### III. EFFICIENCY AND $Q$

To evaluate the antennas' quality factors ( $Q$ ), we must compare them to the fundamental limit. We will compare our antennas to the most practical limit, that for the  $TM_{10}$  mode, from (1). The ratio of the antenna  $Q$  to the limit represents the "optimality" of the antenna in one sense.

Since  $Q_{\min, TM_{10}}$  and the efficiency  $\eta_r$  scale proportionally, we must first determine the radiation efficiency. The radiation efficiency ( $\eta_r$ ) of these antennas is primarily governed by conduction loss, which is closely related to the length of wire. As Fig. 2 shows, the length of wire is significantly greater for the SM antennas than the SH and H. Fig. 4 plots the simulated radiation efficiency versus electrical size, confirming that the SH and H antennas are more efficient than the SM. Furthermore, the SH and H efficiencies degrade less rapidly with a decrease in electrical size. While the efficiencies of the SH and H antennas improve marginally as more arms are added, the efficiency of the SM is lower with more arms because of the significantly increased wire length.

Next, we evaluate the antennas'  $Q$  from their simulated impedance data. There are multiple ways to calculate quality factor. One method uses the frequency derivative of the impedance [2, eq. (96)], which we will call  $Q_Z$ . Another measure of antenna  $Q$  can be calculated from the matched impedance bandwidth [2, eq. (87)], which we call  $Q_{BW}$ . However, this quantity requires additional processing to ensure an

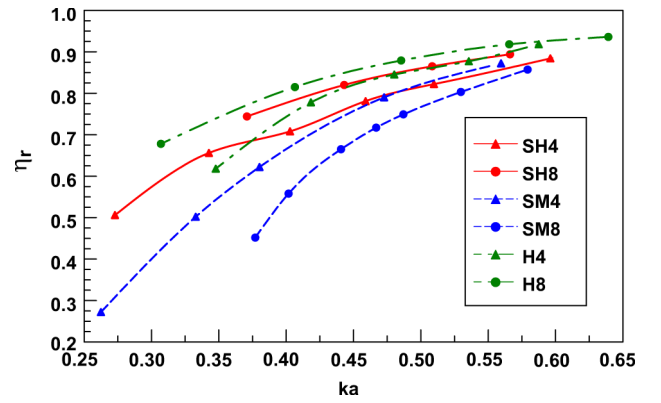


Fig. 4. Simulated radiation efficiency versus electrical size of four- and eight-arm variations of the SH, SM, and H antennas.

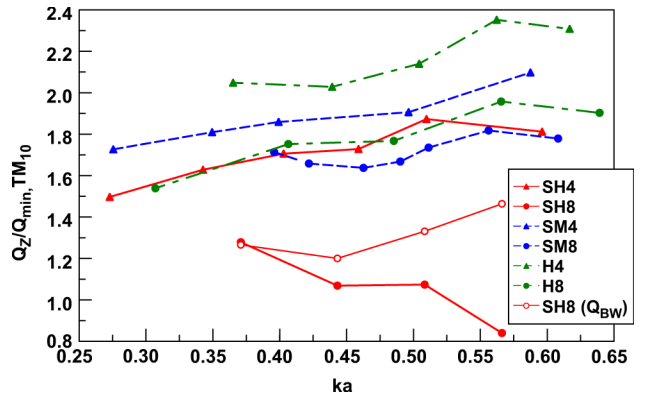


Fig. 5. Ratio of  $Q_Z$  to  $Q_{\min, TM_{10}}$  of simulated four- and eight-arm variations of the SH, SM, and H antennas.  $Q_Z$  is calculated at the center frequency when the antenna has been tuned to operate at the indicated electrical size. For SH8, a factor  $Q_{BW}$  is also calculated from the impedance-matched half-power bandwidth.

ideal impedance match. Both quantities were evaluated for the SH, SM, and H antennas and were found to be equal in nearly all cases. Thus, only the ratio of  $Q_Z$  to the bound is plotted in Fig. 5 for most designs.

Several patterns emerge from Fig. 5. First, it is evident that the designs with more arms have lower  $Q_Z$  relative to  $Q_{\min, TM_{10}}$ . In the designs with more arms, the surface area occupied by the conductor is greater and the  $TM_{10}$  mode is more strongly excited, resulting in a lower  $Q$ . Second, although the efficiency is lower at small electrical sizes, there appears to be little link between the efficiency and the ratio of  $Q$  to the fundamental limit. This limit is proportional to the efficiency from (1), so we can infer that the  $Q$  of the antennas decreases proportionally to the efficiency to yield a constant ratio.

The eight-arm SH has the lowest  $Q_Z$  ratio. However, it is not well matched to 50  $\Omega$ . Because of its large capacitive reactance, it cannot be made self-resonant. Matching the antenna with lumped elements in Agilent ADS, we find that, unlike the other antennas, the  $Q_{BW}$  of the SH8 differs from its  $Q_Z$  value. This divergence, shown in Fig. 5, is due to the presence of an additional mode nearby in frequency to the radiating mode. The quality factors  $Q_Z$  and  $Q_{BW}$  can differ significantly when modes are closely spaced [12]. Thus, it is not clear which measure is most appropriate in the case of SH8, but  $Q_{BW}$  may be

TABLE I  
MEASURED AND SIMULATED ANTENNA PARAMETERS.

Design	$ka$	$\eta_r$		$\overline{Q_Z}$	
		meas.	sim.	meas.	sim.
SH4	0.43	0.73	0.75	1.2	1.7
SM8	0.52	0.61	0.73	2.0	2.0
H8	0.49	0.76	0.85	2.0	1.9

a more useful measure since it is derived from actual performance. A similar multimode response (and impossibly low  $Q_Z$  values) can be observed in the SM antenna if the feed trace is made very wide on a high-permittivity substrate. When properly designed, this phenomenon can be useful for increasing bandwidth [10].

Fig. 5 shows that lower  $Q$  is achieved with more arms. In the case of the SH, this conflicts with our need to choose the number of arms for impedance matching purposes. Thus, the larger bandwidth of the SH antennas must be considered with the increased complexity and loss inherent in a lumped element matching network.

#### IV. FABRICATION OF THE SPHERICAL ANTENNAS

In [7], we demonstrated conformal printing of the SM antenna onto hemispherical glass substrates with maximum dimension as small as 1.3 cm. This is significantly smaller than the SH in [5], which was fabricated manually for operation at 300 MHz with a maximum dimension of about 12 cm. More recently, SH antennas with maximum dimension 3.2 cm have been constructed using a stamping process [13].

Our conformal printing technique enables the fabrication of many complex patterns including the SH, SM, or hybrid designs discussed here. We fabricated the SH4 [Fig. 1(a)], SM8 [Fig. 1(b)], and H8 [Fig. 1(c)] designs on glass hemispheres (outer radius = 12.8 mm and thickness = 1.3 mm). For an impedance match to 50  $\Omega$ , the SM8 and H8 antennas are designed on 0.062-in Duroid 5880 boards, the SM8 and H8 having 0.6- and 1.6-mm-wide copper traces, respectively. The SH antenna is fabricated with only four arms because Fig. 3 indicates that an eight-arm SH design would have maximum return loss of 4 dB. Having chosen the SH4 design and matched the SM8 and H8 using the planar substrate, all three antennas are well matched with return loss at their center frequencies of greater than 15 dB.

The measured SH4, SM8, and H8 antennas have center frequencies of 1.59, 1.72, and 1.63 GHz, respectively, and their other properties are summarized in Table I. As expected from Fig. 4, the SH4 and H8 designs exhibit higher measured efficiency than the SM8, despite its larger electrical size. The  $Q$  of the SH4 is  $1.2\times$  the lower bound defined in (1), while the SM8 and H8 antennas each have a  $Q$  ratio of 2.0. This agrees with the trend in Fig. 5, although the thicker Duroid boards used for the measurements increase the electrical size of the SM8 and H8 antennas, resulting in a higher  $Q$  ratio. Discounting the board thickness, the SM8 and H8 antennas have  $Q$  ratios of 1.4 and 1.5, respectively. Our simulations and experience fabricating these antennas suggest that thinner boards can be used to reduce this effect without noticeably affecting performance.

#### V. CONCLUSION

There are two distinct components in the design process for a small antenna: the design of a resonant, low  $Q$  mode filling a particular volume and the design of an additional inductive or capacitive mode acting as a matching circuit. We have demonstrated both capacitive and inductive matching in this letter and shown that a near-minimum  $Q$ ,  $TM_{10}$  spherical mode can be excited and matched in several ways, with differing  $Q$ , efficiency, and impedance match depending on the details of the geometry.

We have highlighted the differences between the spherical helix and spherical meanderline designs. In particular, the SH has a higher efficiency and lower  $Q$ , but the design may result in an undesirable impedance. It is likely that there are methods to tune the inductive mode of the SH independently of the radiating mode, but these have not yet been demonstrated and are a topic of ongoing investigation.

On the other hand, control of the SM's impedance is straightforward and robust, but the conductor layout on the surface results in a lower efficiency that does not scale well at small sizes. Thus, we introduced a hybrid (H) design that has an efficiency similar or better than the SH as well as excellent control of the impedance. Furthermore, we have shown that these different geometries can be readily fabricated on hemispherical substrates via conformal printing.

#### ACKNOWLEDGMENT

The Duroid substrates were provided by Rogers Corporation.

#### REFERENCES

- [1] H. A. Wheeler, "Fundamental limitations of small antennas," *Proc. IRE*, vol. 35, no. 12, pp. 1479–1484, Dec. 1947.
- [2] A. D. Yaghjian and S. R. Best, "Impedance, bandwidth, and  $Q$  of antennas," *IEEE Trans. Antennas Propag.*, vol. 53, no. 4, pp. 1298–1324, Apr. 2005.
- [3] H. L. Thal, "New radiation  $Q$  limits for spherical wire antennas," *IEEE Trans. Antennas Propag.*, vol. 54, no. 10, pp. 2757–2763, Oct. 2006.
- [4] G. A. E. Vandenbosch, "Reactive energies, impedance, and  $Q$  factor of radiating structures," *IEEE Trans. Antennas Propag.*, vol. 58, no. 4, pp. 1112–1127, Apr. 2010.
- [5] S. R. Best, "The radiation properties of electrically small folded spherical helix antennas," *IEEE Trans. Antennas Propag.*, vol. 52, no. 4, pp. 953–960, Apr. 2004.
- [6] S. R. Best, "Low  $Q$  electrically small linear and elliptically polarized spherical dipole antennas," *IEEE Trans. Antennas Propag.*, vol. 53, no. 3, pp. 1047–1053, Mar. 2005.
- [7] J. J. Adams, E. B. Duoss, T. F. Malkowski, M. J. Motala, B. Y. Ahn, R. G. Nuzzo, J. T. Bernhard, and J. A. Lewis, "Conformal printing of electrically small antennas on three-dimensional surfaces," *Adv. Mat.*, vol. 23, no. 11, pp. 1335–1340, Mar. 2011.
- [8] J. J. Adams and J. T. Bernhard, "Tuning method for a new electrically small antenna with low  $Q$ ," *IEEE Antennas Wireless Propag. Lett.*, vol. 8, pp. 303–306, 2009.
- [9] S. R. Best and J. D. Morrow, "On the significance of current vector alignment in establishing the resonant frequency of small space-filling wire antennas," *IEEE Antennas Propag. Lett.*, vol. 2, pp. 201–204, 2003.
- [10] J. J. Adams and J. T. Bernhard, "A modal approach to the tuning and bandwidth enhancement of an electrically small antenna," *IEEE Trans. Antennas Propag.*, vol. 59, no. 4, pp. 1085–1092, Apr. 2011.
- [11] J. J. Adams and J. T. Bernhard, "Tuning small monopole antennas: Modes, stubs, and  $Q$ ," in *Proc. Antenna Appl. Symp.*, Sep. 2010, pp. 256–269.
- [12] H. R. Stuart, S. R. Best, and A. D. Yaghjian, "Limitations in relating quality factor to bandwidth in a double resonance small antenna," *IEEE Antennas Wireless Propag. Lett.*, vol. 6, pp. 460–463, 2007.
- [13] C. Pfeiffer, A. Grbic, X. Xu, and S. R. Forrest, "New methods to analyze and fabricate electrically small antennas," in *Proc. IEEE Antennas Propag. Int. Symp.*, 2011, pp. 761–764.